

Low-strain integrity testing of rock anchors

H.Mohammed & N.Haritos

The University of Melbourne, Parkville, Victoria, Australia

ABSTRACT: The support of engineering structures such as tunnels, retaining walls, mines, dry docks, dams and pre-stressed structures commonly involves the installation of ground anchorages. Safety is a critical issue for these structures especially for the tunneling and mining industries. Much attention is therefore focused on the integrity of roofs of mining tunnels. One approach is to stabilize the roof with grout or resin anchors. Current testing methods for such anchors are expensive and time consuming. This paper reports the results obtained from integrity testing of rock anchors from low impact blow by analyzing the frequency response curves obtained from acceleration-time trace using the principles of stress-wave propagation theory in steel bars. Laboratory experiments were performed on bolt-grout systems with varying lengths and having predefined defects. An analysis method to determine the free and embedded length of anchor bars in grout is proposed based on the results and experience obtained.

1 INTRODUCTION

Rock bolts are prolifically used as the main support for structures such as tunnels and mines where safety is critical. These bolts are steel rods fixed into the roof with grout to prevent collapse. However their safety might be compromised by poor installation procedures (eg incomplete grout mixing and partially encapsulated bolts), defects associated with bolt corrosion and loss of bond between rock and bolt.

Pull-out testing is the conventional approach for determining rock bolt integrity, but is a destructive and time consuming process. A need therefore has arisen to develop non destructive testing methods to determine the condition of in-situ bolts.

Ultrasonic testing using a device called a Bol-tometer, when used on cement grouted bolts can indicate poor grouting conditions between a rock-bolt and the surrounding rock. However the method has often proved to be unreliable (Kelly et al. 1996).

More recently guided ultrasonic waves have been proposed as a feasible approach for detecting grout defects (Beard & Lowe 2003). When using this method embedded bolts should be tested in both a low frequency range (30-70 kHz) to identify defects such as partial encapsulation and possible corrosion patches on the bolt surface and a high frequency range (2-5 MHz) to indicate bolt length. The technique is a semi-analytical approach and has limitations in simulating complex defect scenarios (Buys

1996). Ultrasonic testing is very expensive, time consuming and may not be feasible for testing hundreds of rock bolts daily at a particular site.

The GRANIT testing system, developed in Scotland, drives a piston that creates a controlled axial impact to the bolt under test. The reflected signals that arise from the impulse are analyzed by a trained artificial neural network (ANN) to identify several types of defects (Starkey et al. 2003). The ANN should be trained by a sufficient number of reflected signals from different types of known defects to improve its effectiveness (Cheung 2003).

Due to limitations in the above systems, there is a need to identify a new simpler method for integrity testing. Halcrow Pacific (tunnel and structural consultants) currently uses the Ground Anchorage Integrity Testing (GRANIT) system for integrity testing of rock anchors and have supported the principal author to conduct research on an interpretive technique that has the potential for providing a simple method to determine 1) the free length of anchor bolts 2) their embedded length and 3) the location of anomalies from cracks in bolts due to corrosion and/or gaps in their grout encasement. This paper reports on progress made towards developing this technique.

2 LITERATURE REVIEW

2.1 Low-strain integrity testing: Theory

Low-strain integrity testing is the examination of response of an element (eg embedded pile) under test, to an external low level mechanical excitation (linear elastic response). The generated compression wave front travels along the pile at a velocity determined by the mechanical properties of the pile material. The resultant wave travels back and forth along the pile leading to occurrences of successive wave interactions at the top end. Thus a number of “reflections” may be detected during the test. The time between any two consecutive arrivals of reflections is related to the distance between the point of reflection and top end of the pile (Davis & Dunn 1974).

2.2 Stress wave propagation in steel bars

The equation of motion for a uniform prismatic bar in axial vibration is given by

$$-C_0^2 \frac{\partial^2 u_1}{\partial y^2} = \frac{\partial^2 u_1}{\partial t^2} \quad (1)$$

The general solution is expressed in terms of two traveling waves each propagating through the rod with wave velocity C_0 , but in opposite directions as

$$u_1 = f_d(x - C_0 t) + f_u(x + C_0 t) \quad (2)$$

where u_1 = elemental displacement at one end of the bar along the bar axis (y); f_d = function representing waves moving down the bar; f_u = function representing waves moving up the bar; t = time, $C_0 = \sqrt{E/\rho}$; E = elastic modulus; and ρ = mass density of the bar.

For a free-ended bar, the stress wave can be followed as a compression wave traveling downward through the bar to the free-ended toe where the stress-wave is transformed to a tensile mode returning to the surface. The tension wave eventually reaches the bar head and pulls the head down towards the toe. Hence a free-end condition results in movement of the bar head in the same direction as that caused by the initial impulse. Conversely, for a fixed-ended bar, when the initial compression wave reaches the bar toe, it rebounds from the rigid elastic surface and the motion is reflected as a compression wave. When the compression wave returns to the surface, the bar head is impelled in the opposite direction to that imparted by the original impulse. Due to changes in impedance, part of the incident wave is reflected and part is transmitted onward. The inference that a return signal detected at the bar head is that from the reflection from toe is determined by considering the distance the wave-front has traveled either from the time lapse between the initial blow and the arriving reflection or from the frequency interval between resonant peaks. From standard wave

theory relating to vibrations in long slender steel rods, the resonating length L is given by

$$L = C_0 / (2\Delta f) \quad (3)$$

where Δf = frequency interval between resonances.

The natural frequency of a steel rod, with both ends either clamped or free, is given by Equation 4. The harmonic number n is replaced with $(n + 1/2)$, if the rod is fixed-free (Tannant & Brummer 1995).

$$f_n = nC_0 / (2L) \quad (4)$$

The steel bar head response is expressed by the parameter V_{max}/F_{max} termed mobility, M . The frequency response curve (frequency as abscissa and mobility as ordinate) therefore takes into account practical variations of the maximum applied force F_{max} which has an effect on the maximum bar-head velocity, V_{max} . The features causing partial reflection of stress-wave will give rise to a characteristic resonance associated with that particular vibrating length and a further resonance associated with the wave traveling to and being reflected from a deeper level. At low frequencies of vibration, the full length of a pile can be discerned and at higher frequencies intermediate impedance changes become increasingly visible. The inverse of the slope of the low-frequency portion of the Mobility curve is a measure of the dynamic head stiffness (Davis & Dunn 1974).

3 EXPERIMENTAL INVESTIGATION

The scope of this investigation is limited to the conduct of experiments for data collection, analysis of frequency domain data for calculating unknown bolt and grout lengths and validation of results by comparison with actual bolt and grout lengths.

3.1 Equipment Used in the Laboratory Experiments

To carry out the experiments 20mm threaded bar bolts ($E=200 \times 10^5$ MPa, density= 7850 kg/m^3 , yield strength= 500 MPa and stress wave propagation velocity= 5045 m/s), were grouted in 100mm ID PVC pipes using Tec grout GP (Non-shrink general purpose grout). A GRANIT field kit comprising a Panasonic CF18 Tough-book laptop, an electronic/battery unit and electro-pneumatic relay valve, a load cell and load indicator, and a solenoid impactor unit from Magnet-Schultz which is a single-acting High-Duty G TC A 040 operating at 24V D.C. was used for impact testing. The impactor unit is fitted with a vibration sensing piezoelectric single-axis accelerometer capable of being sampled at 20 kHz.

The steel bar is connected to the impactor unit during testing by screwing to a nut welded to the unit. The modes of vibration of the steel bar are predominantly axial. The GRANIT recording system

automatically creates a “data file” in which all the response data points are recorded. The system automatically labels the file with the time and date it was created (Littlejohn & Chappell 2005).

3.2 *Experimental Procedure*

3.2.1 *Sample construction*

- 1 The interior of the clean PVC pipes for producing samples for testing were lined with lubricant to allow easy removal after the sample had set.
- 2 A durable tape was used to hold the bolt at the bottom end of the grout encasement and to ensure the pipe cap fitted tightly with no grout leakage.
- 3 To produce a fluid mix, 3.8-4 litres of water were added per 20kg bag of grout. The grout was left for no more than 20 minutes after mixing to achieve full benefit of the expansionary phase.
- 4 Cylindrical grout samples were cast separately for the purpose of performing strength tests.
- 5 Once the pipes had been grouted, the top cap was attached ensuring the bolt remained centralised. The sample was then allowed to set for 270 minutes (initial setting time).

3.2.2 *Investigation setup*

Several different samples with steel bolts embedded in the grout were cast in a cylindrical shape using the vertical PVC pipes as formwork, as described above. A set of four reference test samples cast in this way is shown in Figure 1 by way of example. Each sample aimed to simulate a possible condition scenario of grouted bolts which could occur in the field.

A list of sample types and their description follows:

- 1 Bolt ref.1 – a bolt 600mm long with approximately 400mm grouting representing a situation where the bolt itself may be damaged or broken, so it does not extend the standard 2m length. At the top and bottom ends of the sample, the steel bar protrudes by 150mm and 50mm, respectively.
- 2 Bolt ref.1A – a bolt 600mm long with approximately 450mm grouting demonstrates a situation where the bottom end of bolt is flush with the bottom end of the grout, which means both bolt and grout terminate at the same location along the anchorage. The top end of bar protrudes 150mm.
- 3 Bolt ref.2 – a bolt 1060mm long with approximately 860mm grouting. The protruding lengths at the end are similar to Bolt ref.1.
- 4 Bolt ref.3 – a bolt 1500mm long with approximately 1200mm grouting simulating a damaged state similar to the samples above. However, the end protruding lengths are both 150mm.
- 5 Bolt ref.4 – a fully grouted bolt extending 2100mm with 1800mm grouting, which demonstrates the desired situation - no faults in the anchorage.

- 6 Bolt ref.5 – this sample indicates two situations. One situation being grout leaking out and sinking “partially” to the base of the borehole and the other being a bolt with only a single point support at the bottom. The grouted length is approx. 1525mm and the overall bolt length is 2100mm.
- 7 Bolt ref.6 – similarly to Bolt Ref.5, demonstrates two situations. One situation being grout leaking out and sinking “substantially” and the other being a bolt with only a single point support at the bottom. The grouted length is 500mm. The free length of the bolt is 1450mm and the bolt protrudes 150mm below the bottom.
- 8 Bolt ref.7 – depicts a “partially grouted” situation similar to Bolt ref.5 with a grouted length of approx. 1100mm and a bolt free length of 850mm.
- 9 Bolt ref.8 – involves a gap in the grout. The 200mm gap occurs 500mm from the base and 1100mm from the top.

Bolt ref.1, Bolt ref.2, Bolt ref.3 and Bolt ref.5 were cast on 2nd June, 2009. The acceleration-time GRANIT signals for these samples were recorded on 11th June, 2009. Bolt ref.1A, Bolt ref. 4 and Bolt ref.6 were cast on 23rd June, 2009 and the acceleration time responses were recorded on 21st July, 2009. Bolt ref.7 and Bolt ref.8 were cast on 30th June, 2009 and the responses recorded on 21st July, 2009.

3.2.3 *Sample testing method*

The solenoid impactor was connected vertically to the top end of the test sample (Figure 2) and several impacts (20 repeat tests) were initiated via the field computer using the GRANIT system. Repeatability of the responses was checked by observing the on-screen waveforms. Each sample was impacted at two operating voltages of 26.2V and 45.2V to produce two different impact force levels. The different force levels were selected to investigate whether force level influenced the calculated results.

4 DATA ANALYSIS METHOD

Every impact captured a 2048 acceleration data point time series. Total time required for capturing 2048 data points at a 20 kHz sampling rate is 0.1024 sec.

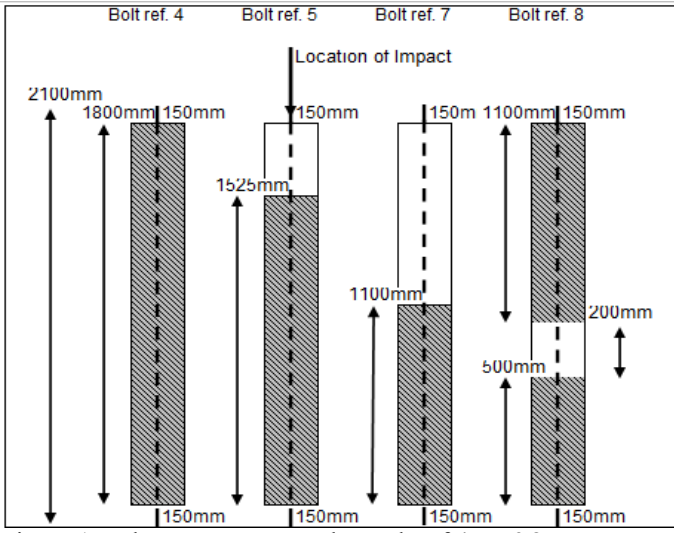


Figure 1. Laboratory test samples Bolt ref.4,5,7&8

The GRANIT system recorded acceleration data at the bolt head to a notepad file on disk inside the field computer and then transferred to an Excel spreadsheet. Such a data trace is a measure of bolt head movement. The impulse travels to the bottom of the steel bar or up to a distance where the stress-wave encounters a sudden impedance change and gets reflected towards the head at a speed and these features are captured in the data trace.

The next step in the data analysis procedure is to convert the acceleration-time data to bolt head velocity by a simple averaging procedure. If a_1 and a_2 are two consecutive acceleration data points over time increment Δt , then velocity V , the area under the acceleration time trace, is calculated from Equation 5,

$$V = \left(\frac{a_1 + a_2}{2} \right) \Delta t \quad (5)$$

A typical velocity time trace for Bolt ref.4 at 45.2V is shown in Figure 3.

The power spectrum function $S(f)$ is then obtained from ensemble averaging of the absolute amplitude squared of the Fourier Transform of N data points of the time history (Cole 1973), given by:

$$S(f) = \frac{1}{N} \lim_{N \rightarrow \infty} \sum_{n=1}^N \frac{2}{T} \left| \int_0^T y(t) e^{-2\pi f t} dt \right|^2 \quad (6)$$

where N = number of data records, T = time length of record in sec, $y(t)$ = amplitude of the time history at time t , t = time instant, and f = frequency in Hz.

The EXCEL algorithm for calculating the discrete Fourier transforms is performed using the complex Fast Fourier Transform (FFT). This routine was applied to both the acceleration and velocity time series data and resultant power spectra then plotted in Excel. The frequency increment is 9.7656 Hz for the data series associated with the samples tested.

The interval distance observed between the frequencies is used to calculate the free and embedded bolt lengths and to determine gaps in the grout. The

discrete form of the Fourier series representation of the time variation function $x(t)$ is represented as

$$x(t) = a(0) + \sum_{n=1}^{N/2} \left(a_n \cos \frac{2\pi n t}{T} + b_n \sin \frac{2\pi n t}{T} \right) \quad (7)$$

$$x(t) = \sum_{n=0}^{N/2} A_n \left(\cos \left(\frac{2\pi n t}{T} - \phi \right) \right) \quad \text{where} \quad (8)$$

$$a_n = \frac{2}{T} \int_0^T x(t) \cos \frac{2\pi n t}{T} dt \quad b_n = \frac{2}{T} \int_0^T x(t) \sin \frac{2\pi n t}{T} dt,$$

a_n, b_n are the Fourier coefficients at $f_n = n/T$, $a(0)=0$ for zero mean, T = total sampling time at regular time step dt of N points.



Figure 2. Bolt-grout samples tested in the laboratory

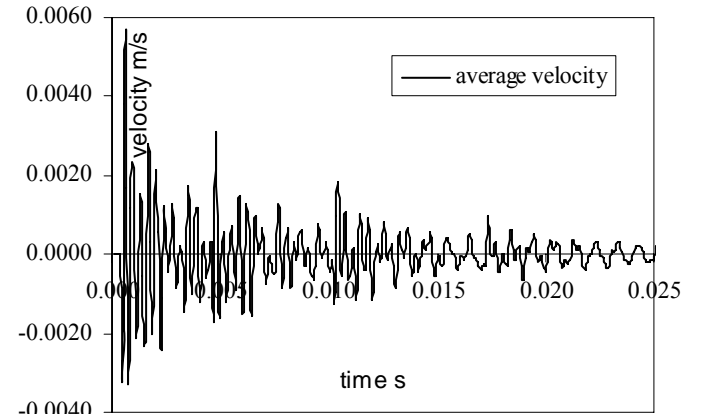


Figure 3. Velocity time trace for Bolt ref.4 at 45.2V

The Amplitude/phase relationships are given by

$$A_n = \sqrt{a_n^2 + b_n^2} \quad \text{and} \quad \phi_n = \tan^{-1} \left(\frac{b_n}{a_n} \right) \quad (9)$$

The power spectrum $S(f)$ is given by

$$S(f) = \left(\frac{a_n^2 + b_n^2}{2} \right) T \quad (10)$$

The velocity power spectrum for Bolt ref.4 is shown in Figure 4.

Substituting Equation 9 for A_n in Equation 8

$$x(t) = \sum_{n=0}^{N/2} \sqrt{2S(f)} df \left(\cos \frac{2\pi n t}{T} - \phi \right) \quad (11)$$

Hence the magnitude of the velocity v from the power spectrum was calculated as

$$v = \sqrt{2S(f)/T} \quad (12)$$

In the spectral density plot, the power at each frequency is proportional to the square of velocity. Once the velocity was evaluated, the velocity-frequency curve was plotted as shown in Figure 5.

The next step in the analysis is to normalize the velocity magnitudes using the maximum applied impulsive bolt force. A Fourier transform was performed to analyze for the amplitudes of the impulsive force, resulting in $a_n=2/N$ and $b_n=0$ for all N .

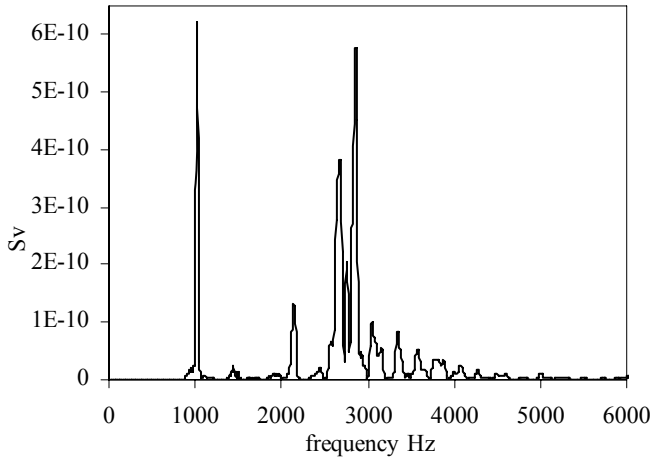


Figure 4. Velocity power spectrum for Bolt ref.4 at 45.2V

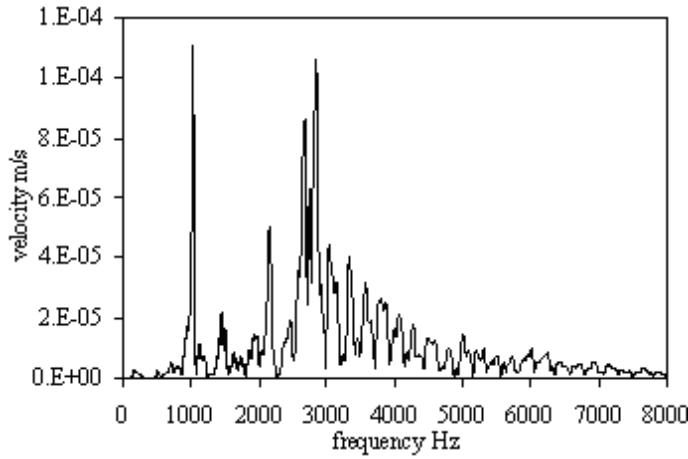


Figure 5. Velocity frequency curve for Bolt ref.4 at 45.2V

In other words, all $N/2$ cosine waves of equal amplitude when added produce the impulsive force. Hence, the impulsive force on the bolt for every frequency increment may be calculated as

$$F_0 = pA/(N/2) \quad (13)$$

where F_0 = maximum impulsive force, p = pressure on the bolt head from the load impactor in N/mm^2 , A = area of cross section of the bolt head in mm^2 , N = total number of captured data points.

Next in the analysis procedure is to plot the mobility curves. The free and embedded lengths may then be calculated using Equation 3.

The properties of the cement grout used in these tests are given in Table 1.

Table 1. Properties of cement grout used in the experiment

Sample	Mean compressive strength	Elastic modulus	Stress wave velocity
	MPa	MPa	m/s
Bolt ref.1	53	32302	3832
Bolt ref.1A	78	39187	4220
Bolt ref.2 & 3	53	32302	3832
Bolt ref.4	78	39187	4220
Bolt ref.5	53	32302	3832
Bolt ref.6	78	39187	4220
Bolt ref.7 & 8 ¹	72	37650	4137
Bolt ref.8 ²	78	39187	4220

¹ top grout strip ² bottom grout strip

The elastic modulus E of the grout is calculated as a function of the mean compressive strength f_{cm}

$$E = \rho^{1.5} (0.043 \sqrt{f_{cm}}) \quad (14)$$

where ρ = density of cement grout (2200 kg/m^3)

The error in estimating the value of "E" is +/- 20%. This affects the estimation of the wave propagating velocity and hence the predicted length. As a result, lengths calculated from mobility curves are expected to vary between 0.9~1.1 x actual lengths.

5 DATA ANALYSIS RESULTS & DISCUSSION

Mobility curves for different bolt grout samples were analyzed for variations in peak frequencies. The mobility curve for Bolt ref.4 is shown in Figure 6.

A summary of the calculated lengths comparison with the measured lengths of the bar and grout is given in Table 2. A typical bolt and grout length calculation (Bolt ref.4) is provided below.

5.1 Length Calculation for Bolt ref.4

The first dominant frequency observed from the mobility curve is 1025.4 Hz. The next higher resonance frequency is 2148.4 Hz. This is understood to be the resonance frequency of the steel bar when the propagating stress waves return to the top of the bar after reflecting from the toe (fixed end). The frequency interval $\Delta f = 2148.4 - 1025.4 = 1123.0 \text{ Hz}$.

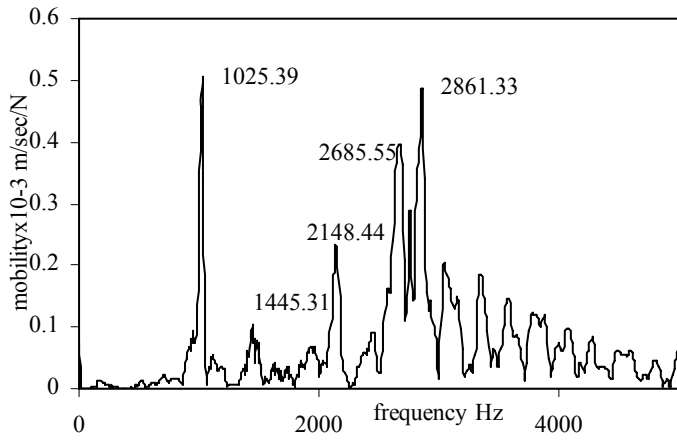


Figure 6. Mobility curve for Bolt ref.4 at 45.V

Table 2. Comparison of lengths of tested bolt-grout samples

Sample	Calculated lengths		Measured lengths	
	Steel bar	Grout	Steel bar	Grout
	m	m	m	m
Bolt ref.4	2.246	1.700	2.100	1.800
Bolt ref.5	2.172	1.475	2.100	1.525
Bolt ref.7	2.172	1.103	2.100	1.100
Bolt ref.6	1.550 ¹	0.818	1.400 ¹	0.500
Bolt ref.8	2.100	1.000 ²	2.100	1.100 ²
Bolt ref.3	1.565	1.270	1.500	1.200
Bolt ref.2	1.100	-	1.060	0.860

¹ protruding length of bar ² grout length above induced defect

The resonating length of the bar L_b is given by

$$L_b = \frac{5045}{(2 * 1123.0)} = 2.246m \quad (15)$$

The measured length of the bar = 2.10m. From the mobility curve, the first predominant grout frequency is 1445.3Hz. The successive dominant resonance frequency is 2685.6 Hz. The resonating length of the grout, L_g is given by

$$L_g = \frac{4220}{(2 * 1539.7)} = 1.70m \quad (16)$$

The measured length of grout in the tested sample = 1.80m. A variation of 10% is expected in the results for the reasons explained in section 4. From the calculations, the calculated lengths of bar and grout are similar to the measured lengths in the laboratory.

The above result for the bar length confirms that for a fully embedded steel bar in grout, the first resonance frequency is due to the individual vibration of the bar. The higher resonance frequencies observed were identified to be from either the vibration of grout around the bar or the vibration of the grout encased length of bar. It is also noted that the second resonance frequency of the steel bar is lower in energy compared to the first. Therefore the lesser the grouted length, the lower the energy attracted by this portion (confirmed from Bolt ref.5 and Bolt Ref.6).

Further examination of the mobility curves of the different samples revealed that the frequencies will have sharp and narrow peaks if either the bar is fully

encased with grout for 1) the full length or 2) with very little or no grout encasement. When the grout encasement is substantial, the grout frequencies become dominant (attract higher energy). As the grout encasement reduces (for Bolt ref.7 grout encasement was almost one-half the length of bar) the frequency band-width near the first resonance frequency of the steel bar widens. This confirms that dominant grout vibration frequency shifts closer to the first bar resonance frequency. With further reduction in grout encasement, the grout frequencies become less dominant and frequency of grout vibration may become less than that of the steel bar vibration due to lower stiffness. It was also inferred that the first resonance frequency of the steel bar reduced when the grout encasement depth decreased due to a gap in the grout sample (Bolt ref.8). But the subsequent grout frequencies became predominant as the encasement was substantial almost up to the bar head. It should be noted that for shorter steel bars with substantial grout encasement, the grout frequencies dominate over the bar frequencies because of the higher combined stiffness of the grout-bolt system (Bolt ref.3). Due to high pass filtering in the data capture, it was not possible to determine the lengths of the shorter bolts as the separation of the steel bar and grout frequencies become extremely difficult to detect.

6 CONCLUSION

Laboratory experiments were conducted for different grouted bolt samples which simulated real life situations with predefined lengths of bolts and grout and the simulated defects in the samples. The proposed method of analysis in the frequency domain using "Stress wave Propagation Theory" can accurately estimate the lengths of bar and grout encasement.

Observed resonance frequencies are sharp and narrow for bars fully embedded in grout or with little encasement and easily identifiable for longer bars (> 2m). Resonance frequencies become well separated with reduced grout encasement. In the case of a short grout encasement (<500mm at bottom) the length of bar up to the grout encasement from the top and the total grout length can be identified using this technique. With gaps in the grout, the total length of bar and the length of grout above the gap can also be identified. For shorter bolt lengths (< 2m), grout frequencies predominate and observed frequencies are not well separated, hence length calculations may prove to be difficult. Unfiltered data capture at a higher sampling rate would be required for detecting lengths of shorter bars. Additional experiments in real rock conditions would need to be performed to verify the accuracy of the proposed method.

REFERENCES

- Beard, M.D. & Lowe, M.J.S. 2003. Non-destructive Testing of Rock Bolts using Guided Ultrasonic waves, *International Journal of Rock Mechanics & Mining Sciences*, 40.
- Buyts, B.J. 2008. Rock Bolt Condition Monitoring Using Ultrasonic Guided Waves, *Report presented to the Faculty of Engineering, Built Environment and Information Technology*, University of Pretoria, South Africa.
- Cheung, W.M. & Lo, D.O.K. 2003. Interim Report on Non-Destructive Tests for Checking the Integrity of Cement Grout Sleeve of Installed Soil Nails: *Special Project Report SPR8*.
- Cole, H.A. 1973. On-line Failure Detection and Damping Measurement of Aerospace Structures by Random Decrement Signature: *NASA Contractor Report CR-2205*.
- Davis, A.G. & Dunn, C.S. 1974. From Theory to Field experience with the Non-destructive Vibration Testing of Piles, *Proc. Institution of Civil Engineers*, 57(2), Dec:571- 593.
- Kelly, A.M. & Jager, A.J. 1996. Critically evaluate techniques for the in-situ testing of steel tendon grouting effectiveness as a basis for reducing fall of ground injuries and fatalities: *Report submitted to SIMRAC*, report No. GAP205.
- Littlejohn, S. & Chappell, M. 2005. Non-destructive Condition monitoring of Ground Anchors, *ADSC Conference on QA/QC and Verification of Drilled shafts, Anchors and Micropiles*, Dallas, Texas.
- Starkey, A. Ivanovic, A. Neilson, R.D. & Rodger, A.A. 2003. Use of neural networks in the condition monitoring of ground anchorages, Elsevier, *Advances in Engineering Software* 34 (2003):753-761.
- Tannant, D.D. & Brummer, R.K. 1995. Rock Bolt behaviour under Dynamic Loading: Field tests and Modelling, *International Journal of Rock Mechanics and Mining Sciences and Geomechanics*, Abstract Vol.32, No.6:537-550.